Available online at www.sciencedirect.com
ScienceDirect
Renewable Energy 32 (2007) 1059–1076
RENEWABLE ENERGY
www.elsevier.com/locate/renene

Technical Note

# Real time estimation of photovoltaic modules characteristics and its application to maximum power point operation

Ausias Garrigós[a,*], José M. Blanes[a], José A. Carrasco[a], Juan B. Ejea[b]

[a] *Área de Tecnología Electrónica, Universidad Miguel Hernández de Elche, Avda. de la Universidad s/n, 03202 Elche, Alicante, Spain*

[b] *Departamento de Ingeniería Electrónica, Universidad de Valencia, Avda. Dr Moliner 50, 46100 Valencia, Valencia, Spain*

Received 16 September 2005; accepted 13 August 2006
Available online 31 October 2006

**Abstract**

In this paper, an approximate curve fitting method for photovoltaic modules is presented. The operation is based on solving a simple solar cell electrical model by a microcontroller in real time. Only four voltage and current coordinates are needed to obtain the solar module parameters and set its operation at maximum power in any conditions of illumination and temperature. Despite its simplicity, this method is suitable for low cost real time applications, as control loop reference generator in photovoltaic maximum power point circuits. The theory that supports the estimator together with simulations and experimental results are presented.


*Keywords:* *I–V* curve estimator; *P–V* curve estimator; Maximum power point calculation; Photovoltaic power systems; Photovoltaic energy

## 1. Introduction

Estimation of the current–voltage (*I–V*) equation parameters is one of the most important tasks performed on solar cells and photovoltaic modules. From a power system designer point of view, the knowledge of these parameters permits to design efficient

*Corresponding author. Tel.: +34 96 665 84 80; fax: +34 96 665 84 97.
*E-mail address:* augarsir@umh.es (A. Garrigós).

0960-1481/$ - see front matter 
doi:10.1016/j.renene.2006.08.004

photovoltaic applications. In industrial environments, these measurements are also crucial in development and production processes. Finally, in power conversion systems, the knowledge of these parameters in real time would permit to control the power flow in the solar array under any condition of irradiation, temperature or degradation of the photovoltaic module. A special case of these systems is the operation at the maximum power point (MPP) that is usually performed by a family of power converters denominated maximum power point trackers (MPPT).

Many techniques have been suggested and used to extract solar cells parameters. Probably, within those methods, curve fitting technique is the most used. The basis of this technique is the determination of solar cells parameters from a wide set of measured coordinates. A higher level of confidence is obtained by applying error analysis and standard deviation calculations to curve fitting techniques as can be seen in [1,2]. In real time applications this method is not suitable due to two main reasons: first, time consumption is quite large, since a high number of coordinates are measured; second, the solar array is swept from short circuit to open circuit condition, which is undesirable or simply impossible from the power converter point of view. Another method proposed is the five point method [1], with this one, the number of sensed coordinates is reduced, but it still uses information from short circuit and open circuit conditions.

The method studied in this work attempts to characterise photovoltaic modules from a simple approximation of the solar cell $I$–$V$ relationship. Obviously, as can be seen later, the fitting confidence over the entire $I$–$V$ characteristic will be usually poor, because crucial parameters are suppressed in the analysis, but the method has some advantages in particular cases. One proposed application is the MPP estimation, dubbed MPPE, which can be used in power control converters to avoid tracking techniques.

The function of a MPPT, in a photovoltaic system (PV) is to create the correct feedback signals in a control loop, in such a way that photovoltaic generators are positioned at a voltage point that draws the maximum power available at any time and with load independence. A large number of methods have been developed to track continuously the MPP in photovoltaic arrays.

A simple attempt to operate a photovoltaic module at its MPP is given in a technique named constant voltage [3]. This technique uses a pseudo MPPT method. The control strategy relies on the intrinsic property of photovoltaic modules that locates the voltage of the MPP ($V_{MPP}$), for monocrystalline silicon modules, close to 76% of the open circuit voltage ($V_{OC}$) of the solar array. In order to obtain the MPP, the power source is disconnected from the rest of the circuit during a short time period. Once $V_{OC}$ is sensed, $V_{MPP}$ is straight forward estimated and it can be used as a reference voltage of the control loop. An analogous technique considers, instead of $V_{OC}$, the short circuit current ($I_{SC}$) [3]. The basic principle of this technique is to consider that the current at the MPP ($I_{MPP}$) is proportional to the short circuit current ($I_{SC}$). Although very simple in conception, disconnecting (or shunting) the solar array is a drawback in the control strategy since a time interval is needed to measure the open circuit voltage (or short circuit current) at every sampling period. Furthermore, the maximum point calculation lies on a linear approximation that finally deals at an operation below the actual MPP.

The perturb and observe [3] method is based on the perturbation of the operating point of a photovoltaic module and the observation of its response in order to obtain the sign of the derivative of power over voltage. The system is constantly perturbed and a power control loop forces the solar array to operate in a condition whose derivative of power over

voltage is zero. A remarkable advantage of this method is its simple implementation, but it has as major drawbacks its inherent oscillating condition around the MPP and the impossibility to track the MPP when atmospheric conditions change rapidly [4], reducing the efficiency.

The incremental conductance method [3,4] compares static and dynamic conductance to track the MPP. As reported in [4] this method is well suited for rapid variations of atmospheric conditions as it has the capability to track with a minimum error the MPP.

For spacecraft power systems, and evolving the idea presented in [5] by considering the electrical model of the solar array, an approach has been proposed in [6]. The basis of the method lies in obtaining the MPP by means of estimating the curve of the solar array in real time.

In this paper is presented a practical development of this approach, from its mathematical derivation to a practical implementation of the estimator. Simulated and experimental results corroborate the validity of the method and its advantages.

## 2. Algorithm description of the MPPE

The MPPE algorithm [6] starts considering the photovoltaic cell as a simplified single diode model whose current vs. voltage characteristic is given in (1). In this model the internal series and parallel resistances are neglected.

$$I = (I_{SC} - I_R(e^{\alpha V} - 1)), \quad \alpha = \frac{q}{AkT}, \tag{1}$$

where $I_{SC}$ is the short circuit current that is proportional to the illumination, $I_R$, is the diode saturation current, $q$ is the electron charge, $k$ is the Boltzmann's constant, $T$ is temperature of the $p$–$n$ junction and $A$ is a shaping factor.

The photovoltaic module equation is extrapolated from $m$ strings of $n$ cells in series dealing to (2)

$$I_{SA} = m(I_{SC} - I_R(e^{(\alpha/n)V_{SA}} - 1)). \tag{2}$$

Assuming this model, the characteristic curve of the photovoltaic module is univocally determined when $I_{SC}$, $I_R$ and $\alpha$ are known.

On the other hand, the derivative of (2) results in (3):

$$\frac{dI_{SA}}{dV_{SA}} = -\frac{m\alpha}{n} I_R e^{(\alpha/n)V_{SA}}. \tag{3}$$

The aim of the algorithm is to estimate the curve using the real time sensing of four coordinates ($p_1$, $p_2$, $p_3$ and $p_4$) from the $I$–$V$ characteristic. From these four points, $I_{SC}$, $I_R$ and $\alpha$ are estimated by doing a linear approximation of the derivative at points $D_1$ and $D_2$ as defined by (4), see Fig. 1.

$$\begin{aligned} V_{D1} &= \frac{V_{p1} + V_{p2}}{2}, \quad I_{D1} = \frac{I_{p1} + I_{p2}}{2}, \\ V_{D2} &= \frac{V_{p3} + V_{p4}}{2}, \quad I_{D2} = \frac{I_{p3} + I_{p4}}{2}. \end{aligned} \tag{4}$$

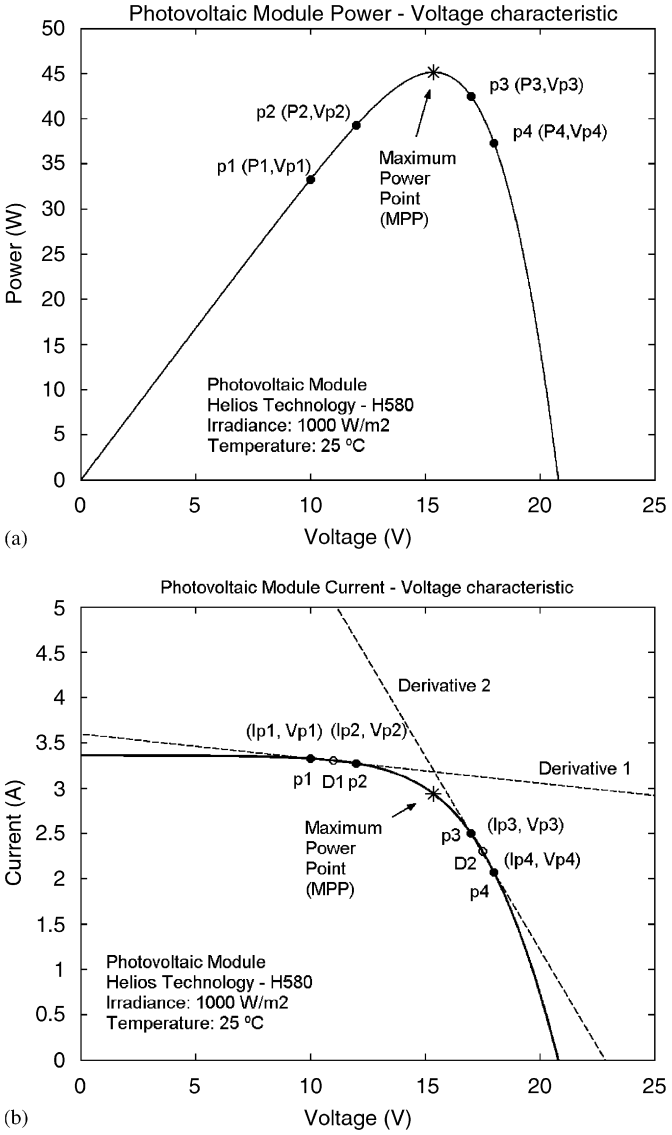


Fig. 1. (a) $P$–$V$ and (b) $I$–$V$ characteristics of a photovoltaic module.

The derivatives of these points are approximated by (5).

$$m_{D1} = \frac{\mathrm{d}I_{D1}}{\mathrm{d}V_{D1}} = \frac{I_{p2} - I_{p1}}{V_{p2} - V_{p1}}, \quad m_{D2} = \frac{\mathrm{d}I_{D2}}{\mathrm{d}V_{D2}} = \frac{I_{p4} - I_{p3}}{V_{p4} - V_{p3}}. \tag{5}$$

Introducing Eq. (5) in (3), the division between the $\mathrm{d}I_{D1}/\mathrm{d}V_{D1}$ and $\mathrm{d}I_{D2}/\mathrm{d}V_{D2}$ results in (6)

$$\frac{m_{D1}}{m_{D2}} = \mathrm{e}^{(\alpha/n)(V_{D1} - V_{D2})}. \tag{6}$$

Applying the logarithm function to (6), the first parameter, $\alpha$ is obtained (7):

$$\alpha = \frac{n}{V_{D1} - V_{D2}} \ln\left(\frac{m_{D1}}{m_{D2}}\right). \tag{7}$$

Once $\alpha$ is estimated, $I_R$ is easily found operating with Eqs. (3) and (5) by substituting them at the point $D_1$ (8):

$$I_R = \frac{-m_{D1} \cdot n}{m\alpha \cdot e^{(\alpha/n)V_{D1}}}. \tag{8}$$

Finally, the short circuit current $I_{SC}$ is found by solving Eq. (2) at point $D_1$ (9).

$$I_{SC} = \frac{I_{D1}}{m} + I_R(e^{((\alpha/n)V_{D1})} - 1). \tag{9}$$

The second part of the algorithm uses the estimated characteristic to obtain the voltage for a specified solar array power applying the Newton–Raphson iterative calculus process. In the particular case that maximum power is pursued, the condition that should be employed is that the derivative of the power over the solar array current equals zero.

Operating in (2), $V_{SA}$ can be expressed as a function of $I_{SA}$ as represented in (10)

$$V_{SA} = \frac{n}{\alpha} \ln\left(\frac{mI_{SC} - I_{SA}}{mI_R} + 1\right) \tag{10}$$

and the power of the photovoltaic module is given by (11)

$$P(I_{SA}) = V_{SA} \cdot I_{SA} = \frac{n}{\alpha} I_{SA} \ln\left(\frac{mI_{SC} - I_{SA}}{mI_R} + 1\right). \tag{11}$$

Since the condition of MPP is $\partial P/\partial I_{SA} = 0$, applying the derivative in (11) gives (12)

$$\frac{\partial P}{\partial I_{SA}} = \frac{n}{\alpha}\left[\ln\left(\frac{mI_{SC} - I_{SA}}{mI_R} + 1\right) - \frac{I_{SA}}{mI_R(mI_{SC} - I_{SA}/mI_R)}\right] \tag{12}$$

and equalling (12) to zero results in the condition for MPP operation. The transcendent equation can be solved by means of the Newton–Raphson [7] method where iteration $j+1$ is given by the result obtained in iteration $j$ as expressed in (13). Note that this method requires an initial condition, in this case, 0.99 times $I_{SC}$ is chosen.

$$\begin{aligned} I_{MPP} &= i(j+1) = i(j) - \frac{f(i(j))}{\partial f(i(j))/\partial i}, \\ f(i) &= \ln\left(\frac{mI_{SC} - i}{mI_R} + 1\right) - \frac{i}{m(I_{SC} + I_R) - i}, \\ \frac{\partial f(i)}{\partial i} &= -\frac{2}{m(I_{SC} + I_R) - i} + \frac{i}{(m(I_{SC} + I_R) - i)^2}. \end{aligned} \tag{13}$$

Once $I_{MPP}$ is known, $V_{MPP}$ is obtained by solving Eq. (10) that results in (14).

$$V_{MPP} = \frac{n}{\alpha} \ln\left(\frac{mI_{SC} - I_{MPP}}{mI_R} + 1\right). \tag{14}$$

## 3. Distribution of the sensed coordinates and seeking algorithm

### 3.1. Relative location of the sensed coordinates

To evaluate the concept just mentioned in the previous section a simulation model of the algorithm proposed is performed in MATLAB, estimated curves have been compared with measured characteristics obtained from an H580 Helios Technology photovoltaic module. An off-line analysis permits to evaluate the sensitivity of the algorithm according to the position of the sensed coordinates.

The error analysis of the fitting procedure is performed using two criteria. The first one gives information on the global approximation of the estimation and it is based on the minimization of the area defined by the difference between estimated and measured curves, $\Delta_{\mathrm{AREA}}$, see Fig. 2. Those areas can be calculated using the trapezoidal rule (15), where $N$ corresponds to the number of sensed coordinates. As reported in [1], minimization of $\Delta_{\mathrm{AREA}}$ will give the best fit over the entire characteristic. Further, the relative error, defined as the coefficient between $\Delta_{\mathrm{AREA}}$ and the area under the measured curve (16), is finally employed to judge the confidence of the estimation. The absolute and relative errors of the short-circuit current (17) and the open-circuit voltage (18) are also useful to observe which part of the $I$–$V$ curve is better approximated.

$$\Delta_{\mathrm{AREA}} \approx \sum_{j=2}^{N} ABS\left\{\frac{(I_{\mathrm{est}}(j)+I_{\mathrm{est}}(j-1)-I_{\mathrm{meas}}(j)-I_{\mathrm{meas}}(j-1))\cdot(V_{\mathrm{meas}}(j)-V_{\mathrm{meas}}(j-1))}{2}\right\}, \tag{15}$$

$$\varepsilon_{\mathrm{AREA}} = \frac{\Delta_{\mathrm{AREA}}}{\sum_{j=2}^{N}\frac{[I_{\mathrm{meas}}(j)+I_{\mathrm{meas}}(j-1)]\cdot[V_{\mathrm{meas}}(j)-V_{\mathrm{meas}}(j-1)]}{2}}, \tag{16}$$

$$\Delta I_{\mathrm{SC}} = I_{\mathrm{SC\,ESTIMATED}} - I_{\mathrm{SC\,MEASURED}},$$
$$\varepsilon_{I_{\mathrm{SC}}} = \frac{\Delta I_{\mathrm{SC}}}{I_{\mathrm{SC\,MEASURED}}}, \tag{17}$$

$$\Delta V_{\mathrm{OC}} = V_{\mathrm{OC\,ESTIMATED}} - V_{\mathrm{OC\,MEASURED}},$$
$$\varepsilon_{V_{\mathrm{OC}}} = \frac{\Delta V_{\mathrm{OC}}}{V_{\mathrm{OC\,MEASURED}}}. \tag{18}$$

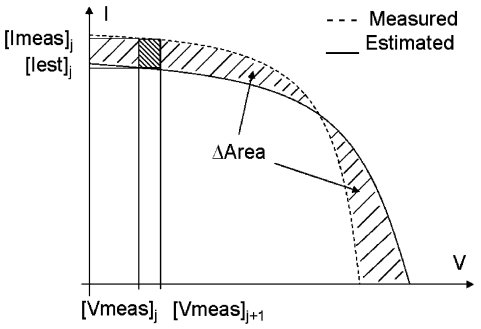


Fig. 2. The area fit criterion schematic (Figure reproduced from [1]).

A second criterion is considered to evaluate the $V_{\mathrm{MPP}}$ estimation. The main parameters calculated in this case are the $V_{\mathrm{MPP}}$ errors (19) and the power errors (20). The power absolute error is defined by the difference between the measured maximum power and the actual power delivered by the photovoltaic module at $V_{\mathrm{MPP\,ESTIMATED}}$.

$$\Delta V_{\mathrm{MPP}} = V_{\mathrm{MPP\,ESTIMATED}} - V_{\mathrm{MPP\,MEASURED}},$$
$$\varepsilon_{V_{\mathrm{OMPP}}} = \frac{\Delta V_{\mathrm{MPP}}}{V_{\mathrm{MPP\,MEASURED}}}, \tag{19}$$

$$\Delta P = P_{\mathrm{MAX}} - P_{\mathrm{VMPP\,ESTIMATED}},$$
$$\varepsilon_P = \frac{\Delta P}{P_{\mathrm{MAX}}}. \tag{20}$$

Finally, the mean and standard deviation of these errors (21) are obtained to reduce the evolution of the solar array characteristics throughout a whole day to a single number.

$$\langle \Delta x \rangle = \frac{1}{M}\sum_{k=1}^{M} \Delta x_k,$$
$$\sigma(\Delta x) = \sqrt{\frac{1}{M-1}\sum_{k=1}^{M}[\Delta x_k - \langle \Delta x \rangle]^2}, \tag{21}$$

where $x$ represents any of the parameters considered in Eqs. (17)–(20) for the $I$–$V$ curve labelled $K$ scanned at a given time and $M$ is the number of $I$–$V$ characteristics acquired during the day.

In order to perform the estimation process, it is necessary to measure four points that will be used to calculate the first parameter $\alpha$. It is apparent that the final estimation is very sensitive to the relative position of each pair of measured points in the $I$–$V$ characteristic.

Taking as reference the measured MPP, there are five possibilities to locate the sensed points into the $I$–$V$ characteristic.

*Case I: Four points below the MPP*. That selection of points fits nicely the current source behaviour part of the curve, as depicted in Fig. 3a, but deals in a poor estimation of the right side of the characteristic because there is no information of the exponential term, and therefore, errors due to series and shunt resistances are magnified. As can be seen in Table 1, the error at the open circuit point can be as large as 10%.

*Case II: Three points below and one point above the MPP*. As represented in Fig. 3b, this case provides an acceptable estimation of the left side of the characteristic, but still lacks precision at the region close to the open circuit voltage.

*Case III: Two points below and two points above MPP*. This option seems to be an optimal trade-off for global fitting. Both current and voltage regions are better fitted according to its actual curve, see Fig. 3c, and it presents the smallest area error.

*Case IV: Three points above and one point below MPP. S*ee Fig. 3d, it offers good performances in the voltage region behaviour and in the MPP estimation but it lacks precision in the current region.

*Case V: Four points above the MPP*. It is represented in Fig. 3e. The main problem lies in a poor estimation of the short circuit current in the most of the cases but, on the other hand, acceptable fitting is achieved at the voltage behaviour part of the curve.

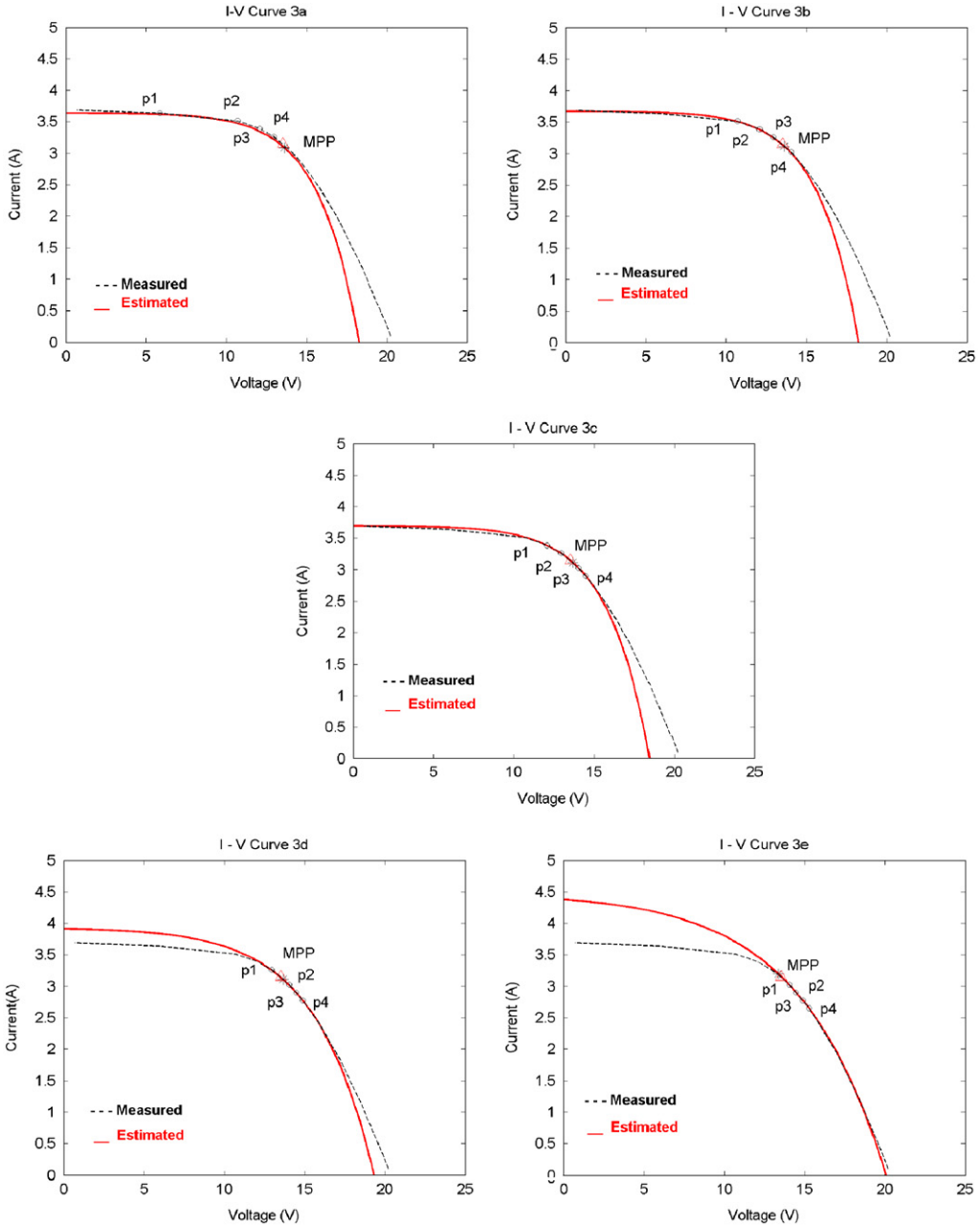


Fig. 3. *I–V* characteristic estimation using five different sets of points. (Δ corresponds to estimated MPP, * corresponds to measured MPP).

Table 1 summarizes the experimental results of the *I–V* characteristics estimation with the five cases described.

Cases *IV* and *V*, which correspond to three points and four points, respectively, above the MPP, can be optimised for an acceptable fitting of the right part of the curve,

Table 1
Experimental results of MPPE algorithm with different selection of sensed $I$–$V$ pairs

| Time | 12:32 | | | | |
|---|---|---|---|---|---|
| Temperature | 47.8 °C | | | | |
| | Case I | Case II | Case III | Case IV | Case V |
| $P_1$—($I_1$, $V_1$) | 3.642 A, 5.855 V | 3.516 A, 10.71 V | 3.387 A, 12.096 V | 3.265 A, 12.941 V | 3.022 A, 14.058 V |
| $P_2$—($I_2$, $V_2$) | 3.516 A, 10.71 V | 3.387 A, 12.096 V | 3.265 A, 12.941 V | 3.022 A, 14.058 V | 2.9 A, 14.488 V |
| $P_3$—($I_3$, $V_3$) | 3.387 A, 12.096 V | 3.265 A, 12.941 V | 3.022 A, 14.058 V | 2.9 A, 14.488 V | 2.77 A, 14.917 V |
| $P_4$—($I_4$, $V_4$) | 3.265 A, 12.941 V | 3.022 A, 14.058 V | 2.9 A, 14.488 V | 2.77 A, 14.917 V | 2.653 A, 15.271 V |
| $I_{SC}$ estimated | 3.6401 A | 3.6783 A | 3.697 A | 3.9098 A | 4.364 A |
| $I_{SC}$ measured | | | 3.695 A | | |
| $V_{OC}$ estimated | 18.2043 V | 18.2006 V | 18.4108 V | 19.2567 V | 19.9821 V |
| $V_{OC}$ measured | | | 20.28 V | | |
| $V_{MPP}$ estimated | 13.6281 V | 13.6236 V | 13.6955 V | 13.6613 V | 13.3605 V |
| $V_{MPP}$ measured | | | 13.545 V | | |
| $P_{MPP}$ estimated | 42.6117 W | 42.6126 W | 42.5975 W | 42.605 W | 42.5271 W |
| $P_{MPP}$ measured | | | 42.6261 W | | |
| $\varepsilon I_{SC}$ (%) | −1.4866 | −0.4521 | 0.0538 | 5.8141 | 18.114 |
| $\varepsilon V_{OC}$ (%) | −10.2353 | −10.2534 | −9.2172 | −5.0456 | −1.469 |
| $\varepsilon V_{MPP}$ (%) | 0.6135 | 0.5799 | 1.1112 | 0.8589 | −1.3623 |
| $\varepsilon P_{MPP}$ (%) | −0.0339 | −0.0318 | −0.0671 | −0.0496 | −0.2324 |
| $\varepsilon$ Area (%) | 5.9109 | 5.0132 | 4.4281 | 4.7792 | 9.021 |

preserving, at the same time, small error in MPPE. This feature is potentially useful in power flow control of the solar array. The voltage region of the $I$–$V$ curve shows a high sensitivity of power over voltage, and a small variation of the voltage reference produces a considerable variation of the power extracted from the solar array. Considering this property, a DC bus voltage can be fixed between the voltage in the MPP and the voltage in the open circuit point and the entire power of the solar array can be controlled.

An important consideration derived from a first observation of the results presented in Table 1 is that the $V_{MPP}$ error is kept low with independence of the position of the sensed coordinates. As can be seen in Fig. 4, it is hard to appreciate the difference between the positions of the $V_{MPP}$ obtained with the five possible distributions of the sensed points. Even taking into account the deviations respect the measured MPP, the power difference from maximum power is very small, usually less than 0.3%. The main derivation of this result is that high precision MPP estimation can be achieved with independence of the location of the sensed coordinates. In MPP applications this situation is advantageous since tracking process is avoided; just a few measurements around any operating point are needed before computation of the new MPP.

### 3.2. Seeking algorithm for distribution of the sensed points

Although the MPPE application seems to be independent of the location of the sensed coordinates, a simple seeking algorithm can be implemented to offer, besides, better fitting over the entire $I$–$V$ characteristic. This algorithm forces the system to operate in *Case III*, which will result in the best global fitting. Experimental confirmation is summarized later in Table 2.

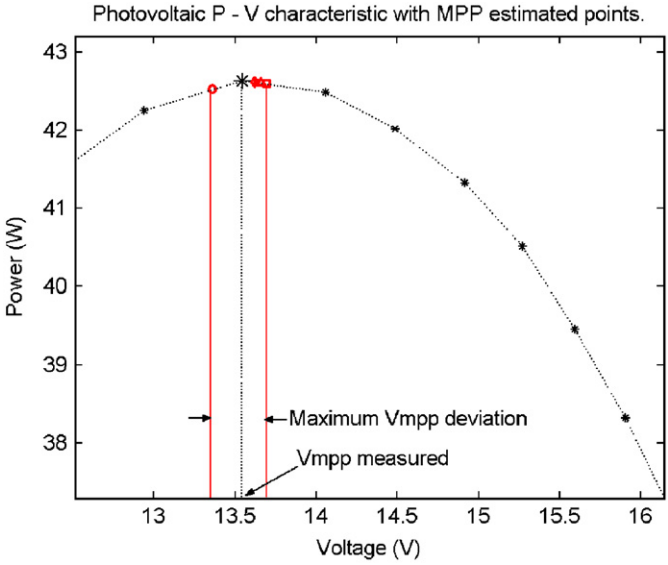


Fig. 4. Detail of the $P$–$V$ characteristic with the estimated MPP obtained by the five possible distribution of the sensed points.

Table 2
Mean and standard deviation of the main parameters considering a whole day evolution

| Mean/Standard deviation | | | | | |
|---|---|---|---|---|---|
| | $\langle \Delta I_{sc} \rangle / \sigma(\Delta I_{sc})$ | $\langle \Delta V_{oc} \rangle / \sigma(\Delta V_{oc})$ | $\langle \Delta V_{mpp} \rangle / \sigma(\Delta V_{mpp})$ | $\langle \Delta P \rangle / \sigma(\Delta P)$ | $\langle \Delta_{Area} \rangle / \sigma(\Delta_{Area})$ |
| Case I | −33.5 mA/24.4 mA | −1.0263 V/837.4 mV | 140.5 mV/250.1 mV | −62.8 mW/97.2 mW | 3.9463 W/1.6229 W |
| Case II | −22.2 mA/25.6 mA | −1.5 V/433.8 mV | −31.4 mV/171.8 mV | −19 mW/21.3 mW | 4.1379 W/1.4051 W |
| Case III | −34.5 mA/43.3 mA | −1.5522 V/270.4 mV | 11.8 mV/165.4 mV | −22.7 mW/20.3 mW | 4.3368 W/1.0667 W |
| Case IV | 54.3 mA/87.3 mA | −1.1959 V/232.6 mV | −28.6 mV/180.1 mV | −19.5 mW/17.8 mW | 3.9997 W/1.0493 W |
| Case V | 280.4 mA/209.5 mA | −0.8069 V/349.1 mV | −200.5 mV/260.2 mV | −70.4 mW/74.5 mW | 6.4849 W/2.4180 W |

The algorithm used in this work is based on producing controlled voltage steps in the photovoltaic module voltage, and then, comparing the power obtained with the previous measurement. Knowing the direction of the voltage step and the sign of the power difference between the two points it can be determined to which region, constant current or constant voltage, the sensed coordinate belongs. Fig. 5, shows a simplified example of the proposed seeking method. At some instant, the solar array voltage is given by $V_{BUS}$ and a condition for starting a new estimation appears. That condition is given by a variation of the current in the photovoltaic module above a threshold. At start, $V_0$ equals $V_{BUS}$ and the estimation algorithm begins. A positive voltage step, $\Delta V_1$, is produced; if the power measured is less than $P_0$ the new point has negative $dP/dV$ and it is a valid coordinate; this coordinate is $p_3$. Then, a new positive voltage step is produced, $\Delta V_2$, and $p_4$ is obtained. After that, a negative voltage step is produced, $\Delta V_3$; if the new coordinate has a power, $P_x$, greater than $P_0$ then it can not be concluded whether $dP_x/dV$ is negative or positive, and

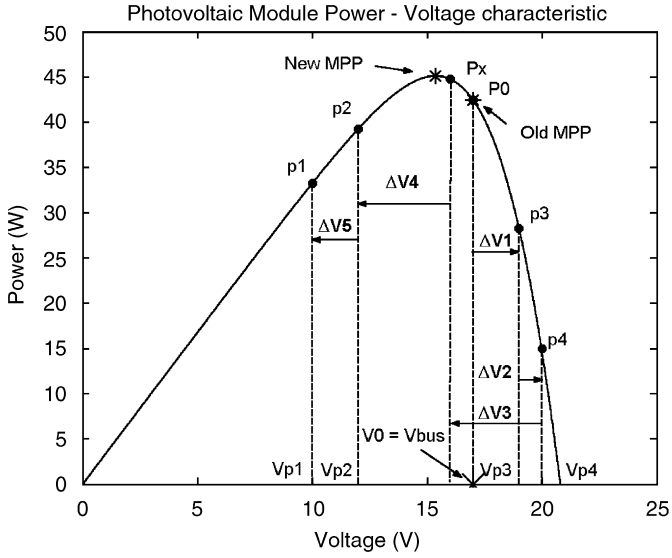


Fig. 5. Description of the seeking algorithm described in text.

therefore it could not be valid coordinate. A fourth voltage step, $\Delta V_4$, is applied; if the new coordinate has a power, $P_2$, less than $P_X$, then we have a positive $dP/dV$ and a new valid point, $p_2$. The last coordinate, which has a power $P_1$, is obtained by producing a negative voltage step, $\Delta V_5$ and sensing the current and voltage of the photovoltaic module. A complete flowchart of the algorithm is found in Fig. 6.

## 4. Experimental validation and discussion

An experimental validation workbench has been implemented as follows. A Helios Technology H580 photovoltaic module is characterised by means of a PC based system with a LABVIEW software application, see Fig. 7a. This instrumentation setup is continuously sweeping the solar array module, by means of a DC electronic load, and saving the *I–V* curves into PC files. The values obtained in those curves are used to evaluate the proposed algorithm and to find the MPP in real time at actual temperature and irradiance conditions.

An identical H580 photovoltaic module is controlled by a low cost microcontroller system, as depicted in Fig. 7b. In that system, the seeking and estimation algorithms have been implemented following the description at Section 3.2. The microcontroller controls a DC electronic load working in voltage mode that performs the functions of a DC bus of a photovoltaic power converter. Time domain evolution of the bus voltage permits to validate the concept proposed and to estimate the essential parameters.

The DC electronic load [8] is implemented by two power mosfet transistors operating in its linear region while an analogue feedback loop controls the voltage across the transistors. The reference of the control loop is provided externally by the PC or the D/A converter in the case of microcontroller based system, see Fig. 8.

The microcontroller based system can be observed in Figs. 7b and 9. It consists on a low cost microcontroller, Microchip Technology PIC18F252, programmed with the seeking and

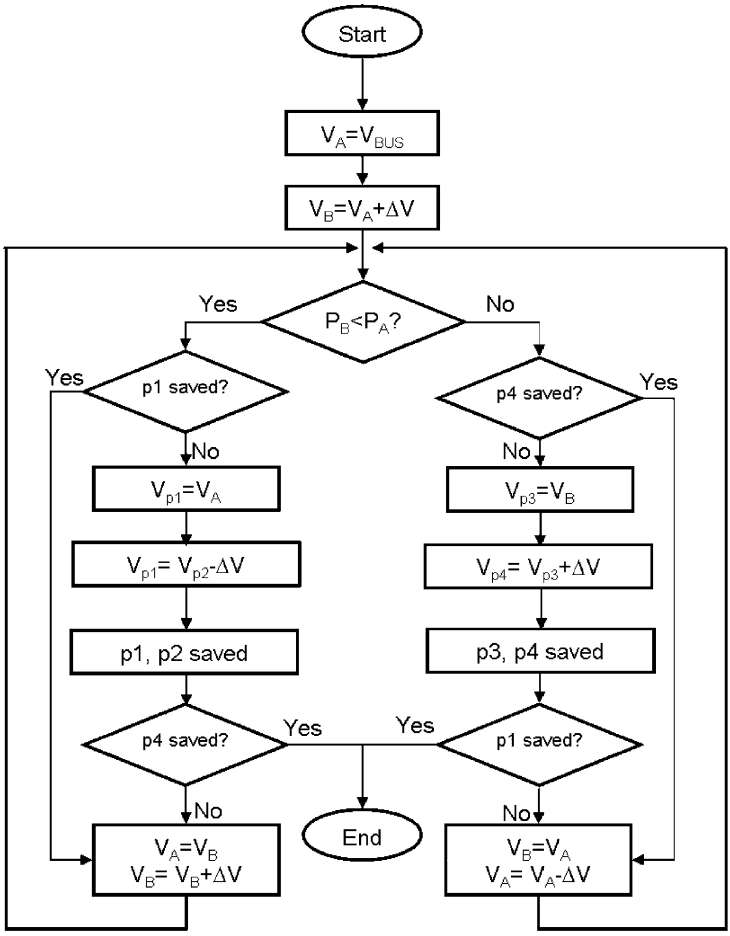


Fig. 6. Flowchart of the seeking algorithm needed to sample the *I–V* characteristic.

estimation algorithms. The solar array voltage and current are sensed by a simple voltage divider and a Hall effect current sensor, an Allegro Microsystems ACS750. Sensed points are converted into digital signals through two A/D 10-bit converters, which are internal to the microcontroller. The DC electronic load is remotely controlled by a 12-bits D/A converter, Microchip Technology MCP4921. The system also offers a wireless replacement of a standard RS232 interface over the Bluetooth Serial Port Profile [9] by using a Taiyo Yuden EYMF2CAMM-XX module. This Bluetooth interface offers isolation and operation or monitoring of the MPP system from a remote computer (up to 100 m).

## 5. MPPE experimental validation

Tests performed on the MPPE algorithm are organised as follows: the first test, as discussed in Section 3, is customized to observe the effect of the different location of the sensed coordinates. The results are summarized in Fig. 3 and Table 1. The next step is an

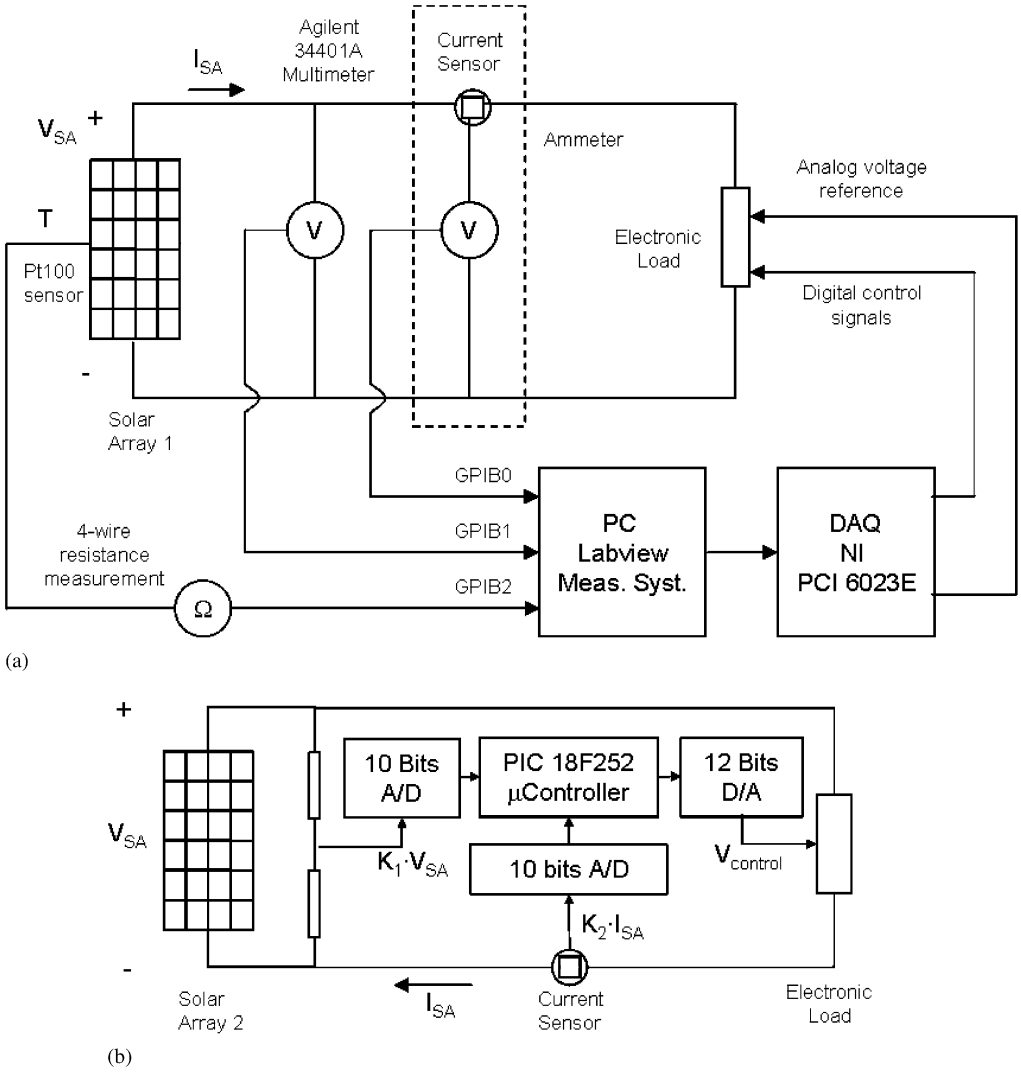


Fig. 7. Experimental setup diagram: (a) PC; and (b) microcontroller setups.

on-line setup that registers continuously the *I–V* characteristics of a photovoltaic module during one whole day and executed the MPPE algorithm with the points sensed in a personal computer running LABVIEW to corroborate its validity. Tests were done in February 17th at Elche, Spain, in winter season and a sunny day from 10:00 to 15:00. A diagram of the setup employed is shown in Fig. 7a. Fig. 10 represents the evolution of the main parameters in the estimation process. The distribution of coordinates chosen is two points below and two points above the MPP.

Finally, in Table 2 the mean and the standard deviation of the main errors are represented for the measurements made during that day and considering the five possibilities of distribution of points within the *I–V* characteristic.

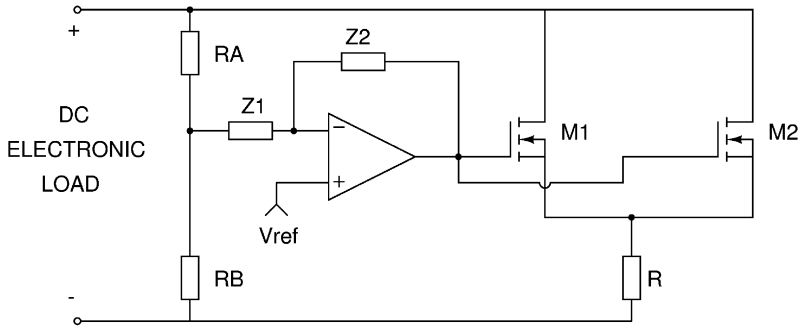


Fig. 8. DC electronic load schematic diagram.

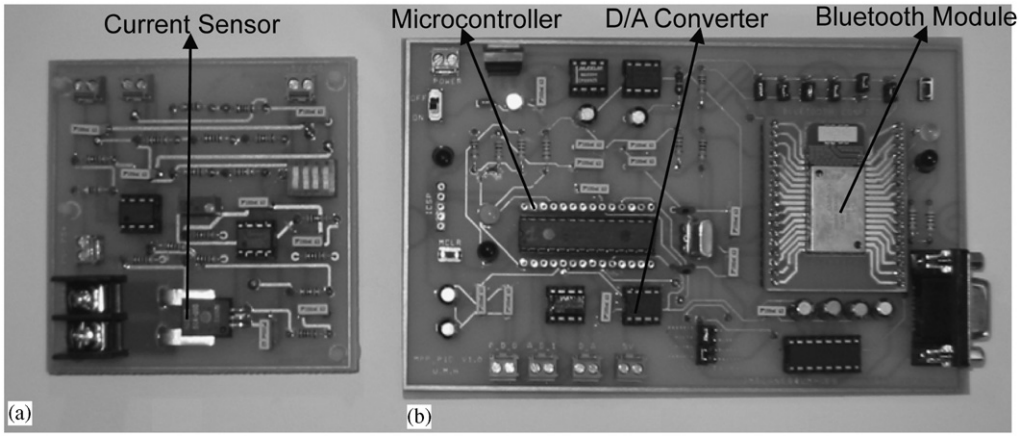


Fig. 9. (a) Current and voltage sensing board photograph, (b) microcontroller based estimator photograph.

It is interesting to note that in all cases the power error is kept very low; mean and standard deviation are less than 100 mW and that corroborates its applicability to MPPE. On the other hand, Table 2 also shows that the election of four coordinates above $V_{MPP}$ is the best choice for fitting the right part of the $P$–$V$ characteristic, but lacks precision in short circuit current estimation. Analogous results are obtained considering four points below $V_{MPP}$. Finally, the other three possibilities, three, two and one point below points below $V_{MPP}$ do not show any significant difference between them, and the power losses due to errors in the estimation is almost the same as well as the area error fitting in all cases.

## 6. Microcontroller based system verification

In these tests the time domain evolution of the solar array voltage and current is represented. Fig. 11 shows the detailed process of the seeking and estimation algorithms. The system remains at a fixed operating point, labelled by (a) in Fig. 11, until a variation of the current in the photovoltaic module occurs. This variation is fixed by a hysteresis of around 35 mA that represents the 1% of the short circuit current at nominal irradiance and

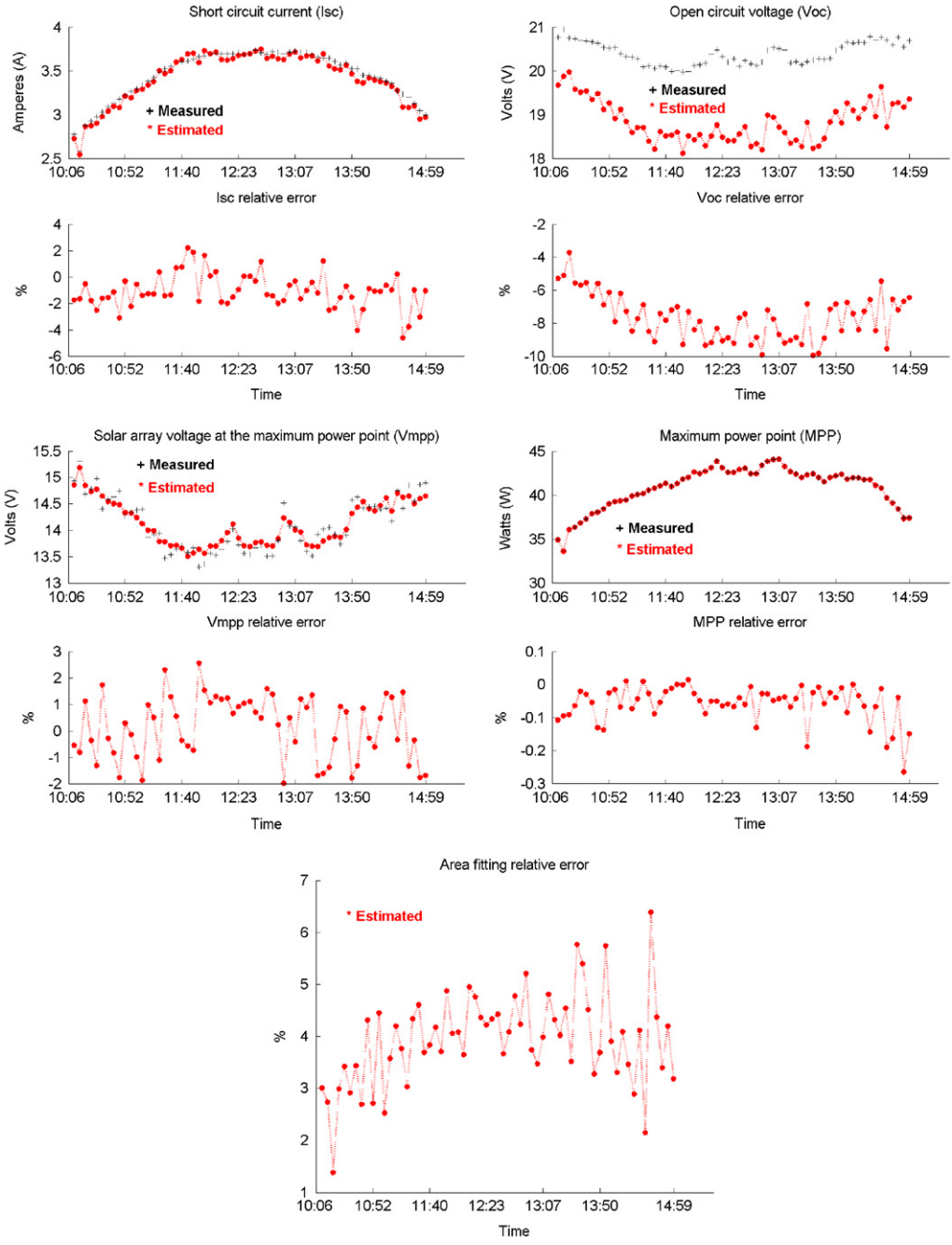


Fig. 10. Experimental validation of proposed algorithm. Error representation of the main parameters considering a whole day.

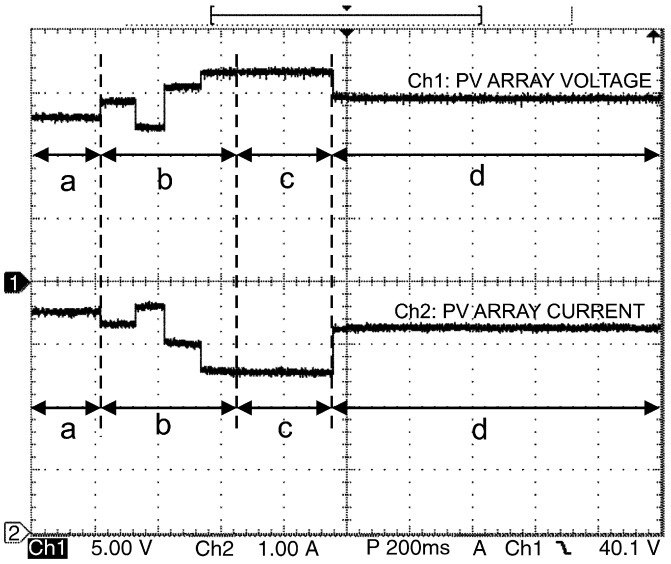


Fig. 11. Time domain evolution of proposed MPPE algorithm. Detailed oscillograph.

temperature conditions. The voltage step is initially fixed at one volt and it is incremented during the seeking process if valid coordinates are not found. At the beginning of zone (b) this condition is detected and the seeking algorithm is started; Valid *I–V* points are saved in the microcontroller during (b) and used later in the estimation process. In zone (c) the system remains in its last state used in the seeking process and all parameters for the new MPPs are calculated. After the estimation the system varies the DC electronic load stabilising the bus voltage to the new MPP. The time consumed during the estimation process involves 450 ms for seeking and 300 ms for calculation of all solar array parameters and the new $V_{MPP}$. Those times can be reduced if the seeking process is substituted by any four steps without forcing the points to fulfil Case III; then, the total consumption will be less than 400 ms. These times are based to a 20 MHz 8-bit microcontroller.

Fig. 12 shows a longer time evolution with different illuminating conditions. Partial shadings are artificially produced by walking in front of the photovoltaic module. As observed in Fig. 12, four estimation processes occurred during shading intervals and finally a last change is produced by a variation of the nominal illumination conditions. In the figure, $S(n)$ refers to a seeking process of the four valid points, $E(n)$ refers to a estimating process and $M(n)$ refers to MPP positioning.

Finally, the PROS, the CONS and POTENTIAL APPLICATIONS of the method are summarised afterwards:

- PROS
  - Simple method to obtain the parameters of a solar cell or photovoltaic module with independence of illumination, temperature, aging or any other degradation effects.
  - It exhibits a high versatility when compared with the traditional methods (e. g. perturb and observe or incremental conductance), since not only calculates the MPP voltage like the traditional methods do, but it adjust the whole *I–V* or a part of it.

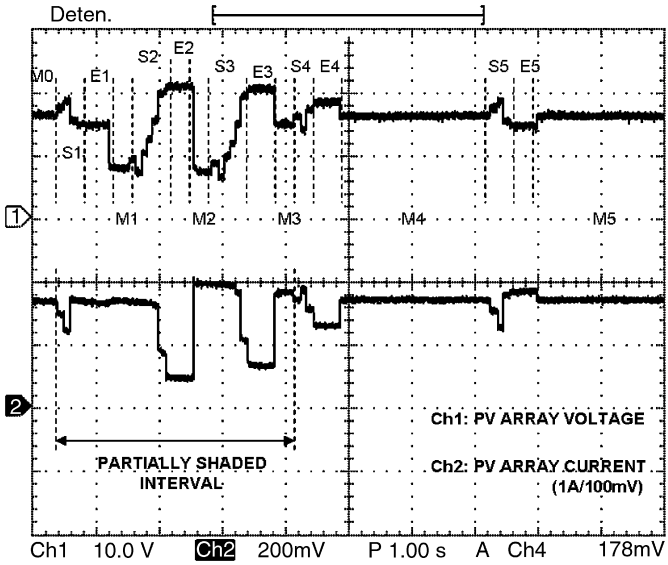


Fig. 12. Time domain evolution during high variable conditions. 1 s/div time scale, due to partially shading of the photovoltaic module.

- Easily adaptable to low cost microcontroller or DSP based system.
- Computationally simple enough to be implemented in real time systems.
- Neither short circuit nor open circuit points are used.
- High confidence in MPPE.
- The method easily replaces the MPPT control strategy by a MPPE. This estimator controls the dc–dc converter that maintains the correct voltage at the solar array, to make it work at its MPP.

- CONS
  - The method, due to the simplicity of the model, lacks precision over the entire $I$–$V$ characteristic fitting and it is quite sensitive to the location of the sensed coordinates.
  - In very low cost systems the impact of the estimator can be significant.
- POTENTIAL APPLICATIONS
  - Control loop reference generator for photovoltaic MPPs applications.
  - The knowledge of the $I$–$V$ or $P$–$V$ characteristic permits a direct control of the power source, e.g. a control system could set a voltage in such a way the solar array would draw a predefined power. From this point of view, MPP operation would be a particular case of this approach.

## 7. Conclusions

In this paper, a novel microcontroller based system to estimate the MPP of solar arrays without tracking process (MPPE) has been simulated and implemented. The estimator changes the operating point of the solar array until it is able to estimate its characteristic curve and therefore compute its MPP coordinates. Although the estimated curve is quite

sensible to the position of the four sensed points, the MPP estimation is accurate enough for real time applications and it can replace MPP tracking techniques. Good agreement between simulated and experimental results is presented to validate the concept. The results show the outstanding performance of MPPE based on a real-time algorithm that may be implemented in a low cost 8-bit microcontroller.

## References

[1] Chan DSH, Phillips JR, Phang JCH. A comparative study of extraction methods for solar cell model parameters. Solid-state electroncs 1986;29(3):329–37 Pergamon Press Ltd.
[2] Haouari-Merbah M, Belhamel M, Tobías I, Ruiz JM. Extraction and analysis of solar cell parameters from illuminated current–voltage curve. Solar Energ Mater Solar Cells 2005;87:225–33.
[3] Hohm DP, Ropp ME. Comparative study of maximum power point tracking algorithms. Progr. Photovolt: Res Appl 2003;11:47–62.
[4] Hussein KH, Muta I, Hoshino T, Osakada M. Maximum photovoltaic power tracking: an algorithm for rapidly changing atmospheric conditions Generation. Trans Distrib IEE proc 1995;142(1):59–64.
[5] Altas IH, Sharaf AM. A novel on-line MPP search algorithm for PV arrays. IEEE Tran Energ Conversion 1996;11(4):748–54.
[6] A. Capel, Circuit de conditionamient pour une source de puissance au point de puissance maximum, generateur solaire et procede de conditionnement, French patent, FR 2 844 890—A1, March 2003.
[7] Press WH, Vettering WT, Teukolsky SA, Flannery BP. Numerical recipes in C: The art of scientific computing, 2nd ed. Cambridge: Cambridge University Press; 2002 Chapter 9, pp. 362–367.
[8] Garrigos A, Blanes JM. Power MOSFET is core of regulated-dc electronic load. EDN 2005:92–3.
[9] Gratton DA. Bluetooth profiles. The definitive guide. Englewood Cliffs, NJ: Prentice-Hall; 2003.